Center for Turbulence Research
Proceedings of the Summer Program 1992

Investigation of the dilatational dissipation in compressible homogeneous shear flow

By G. A. Blaisdell[1] AND O. Zeman[2]

The dilatational dissipation rate within compressible homogeneous turbulent shear flow is studied using data from direct numerical simulations. It is found that the dilatational dissipation rate is mainly associated with large scale acoustic waves. Eddy shocklets are observed; however, they have little contribution to the average dissipation rate. A mechanism for the generation of eddy shocklets is shown to be the focusing of acoustic waves. Turbulence models for the dilatational dissipation rate are compared with data from the simulations. It is found that the formulation of Zeman (1990) used by Viegas & Rubesin (1991) to calculate a compressible mixing layer agrees well with the numerical simulation results for turbulent Mach numbers less than 0.3. However, it is also found that, for the Mach number range occurring in mixing layers, the model does not accurately represent the theory upon which it is based.

1. Introduction

Compressibility effects on turbulence are important in several applications including hypersonic and supersonic boundary layers, scramjet and ramjet engines, and internal combustion engines. The accurate and reliable prediction of such flows requires improvements be made to current turbulence models. Our goal is to better understand compressible turbulence and to make improvements to turbulence models for compressible flows. The approach used is to examine results from direct numerical simulations (DNS) of compressible homogeneous turbulent shear flow.

Direct numerical simulations of compressible homogeneous turbulent shear flow by Blaisdell *et al.* (1991) and Sarkar *et al.* (1991a) have shown that the growth rate of turbulent kinetic energy is reduced compared to the incompressible case. The reduction in the growth rate has been attributed to two additional compressibility terms occurring in the turbulent kinetic energy equation — the dilatational dissipation rate and the pressure-dilatation correlation. The dilatational dissipation rate is an additional dissipation due to the divergence of the velocity, while the pressure-dilatation correlation represents a reversible transfer of energy between internal and kinetic energy. Turbulence models for both of these terms have been proposed by Zeman (1990, 1991) and by Sarkar *et al.* (1991b, 1992). In the current investigation only the dilatational dissipation rate is considered.

1 Purdue University
2 Center for Turbulence Research

The basis for the models of Zeman (1990) and Sarkar *et al.* (1991b) are very different. Sarkar's model is based on the idea of acoustic equilibrium while Zeman's model is based on the existence of eddy shocklets. The direct numerical simulations of Blaisdell *et al.* show the existence of eddy shocklets, which are regions of strong local dilatational dissipation rate. In spite of this, Sarkar's model was found to agree better with the DNS data than Zeman's model. However, a comparison by Viegas and Rubesin (1991) of the two models applied to a compressible mixing layer showed that Zeman's model performed better in predicting the reduction in growth rate with increasing convective Mach number. Therefore, we seem to have contradictory evidence on the relative merits of the two models. It will be shown that the reason for the differences in the comparisons is that the model formulations considered are different.

The objectives of the present work are to shed some light on the apparent discrepancy in the relative performance of the two turbulence models and to better understand the dilatational dissipation in compressible homogeneous shear flow. We begin by examining the formulation of Zeman's model.

2. Model formulations for the dilatational dissipation rate

In both the models of Zeman (1990) and Sarkar *et al.* (1991), the dissipation rate in a compressible flow is written as

$$\varepsilon = \varepsilon_s + \varepsilon_d = \varepsilon_s(1 + \varepsilon_d/\varepsilon_s) \tag{1}$$

where ε_s is the solenoidal dissipation rate and ε_d is the dilatational dissipation rate. For homogeneous turbulence the solenoidal dissipation rate is given by $\varepsilon_s = \widetilde{\mu\omega_i'\omega_i'}$, where ω_i' is the fluctuating vorticity. This is the same as the dissipation rate in an incompressible flow. The dilatational dissipation rate is $\varepsilon_d = (4/3)\widetilde{\mu d' d'}$ where $d' = \partial u_i'/\partial x_i$ is the divergence of velocity (also called the dilatation). Both Zeman and Sarkar *et al.* have suggested modeling ε_s in the same manner that the dissipation is modeled in incompressible flows while accounting for compressibility effects through the ratio $\varepsilon_d/\varepsilon_s$. This strategy is supported by examination of the turbulent kinetic energy budget in the simulations of Blaisdell *et al.* (1991).

The model of Sarkar *et al.* is based on the idea of acoustic equilibrium between kinetic and internal energy and assumes a certain variation of the pressure variance with turbulent Mach number. The model is

$$\varepsilon_d/\varepsilon_s = c_s M_T^2 \tag{2}$$

where $M_T = q/\widetilde{a}$ is the turbulent Mach number, $q = \sqrt{\rho u_i'' u_i''/\overline{\rho}}$ is the turbulent velocity scale using the Favre fluctuating velocity, and $\widetilde{a} = \sqrt{\gamma R\widetilde{T}}$ is the speed of sound based on the Favre averaged temperature. The model constant $c_s = 1.0$.

The model of Zeman (1990) is based on the existence of eddy shocklets and is formulated in terms of the probability density function (PDF) of the fluctuating

Mach number. An expression for the dilatational dissipation is given in equation (7) of Zeman (1990) which is then put in the form

$$\varepsilon_d/\varepsilon_s = c_z F(M_t^*) \,. \tag{3}$$

Zeman uses a turbulent Mach number, M_T^*, which is based on sonic conditions. The sonic temperature is given by $T^* = T_0[2/(\gamma+1)]$ where T_0 is the stagnation temperature. Zeman argues that T_0 can be replaced by the Favre averaged static temperature, $\tilde{T}$. Then the turbulent Mach number used by Zeman can be related to that used by Sarkar *et al.* by

$$M_T^* = \frac{q}{\sqrt{\gamma R T^*}} = \sqrt{\frac{\gamma+1}{2}}\frac{q}{\sqrt{\gamma R \tilde{T}}} = \sqrt{\frac{\gamma+1}{2}} M_T \,. \tag{4}$$

For the case of a diatomic gas, $\gamma = 1.4$ and $M_T^* = 1.10 M_T$. (Throughout the current paper use is made of M_T and M_T^* as well as M_{rms}. These are referred to as the turbulent Mach number, the turbulent Mach number based on sonic conditions, and the *rms* Mach number respectively. Data from the DNS show that M_T and M_{rms} differ by less than 1% and, therefore, can be used interchangeably.)

In determining $F(M_T^*)$, the form of the PDF varies depending on the flow considered. A form appropriate for homogeneous turbulence is given in equation (5) of Zeman (1991). This is the form used in the comparison of Blaisdell *et al.* (1991). The comparison of $\varepsilon_d/\varepsilon_s$ is shown in figure 1. The DNS results are indicated by the symbols. For a given initial *rms* Mach number, $\varepsilon_d/\varepsilon_s$ develops to become independent of its initial value, and the asymptotic values are the ones that should be compared to the model. The model results are shown by the dotted curve. In comparison to the DNS results, the model predicts too fast an increase with turbulent Mach number, and it underpredicts the values at low M_t. The model of Sarkar *et al.* (1991b) is also shown in figure 1. It matches the DNS data fairly well. On the basis of this comparison, one would conclude that Sarkar's model is better.

For compressible mixing layers, Zeman (1990) uses a PDF parameterized by the kurtosis of the fluctuating Mach number, K, as shown in equation (6) of that paper. Different values of K give different relations for $F(M_t^*)$, as shown in figure 2 of Zeman (1990). Rather than choose a particular value of K for performing calculations, Zeman (1990) offers a curve fit as follows

$$F(M_t^*) = \begin{cases} 1 - \exp\{-[(M_t^* - 0.1)/0.6]^2\}, & \text{if } M_t^* > 0.1; \\ 0, & \text{if } M_t^* \le 0.1. \end{cases} \tag{5}$$

This is the form used by Zeman (1990) and by Viegas & Rubesin (1991) to calculate the compressible mixing layer. It was found to give good results for the reduction in the growth rate with convective Mach number. Even though this formulation was developed for the mixing layer, it is interesting to compare it with the homogeneous shear flow DNS data. This is also shown in figure 1. The above formula fits the

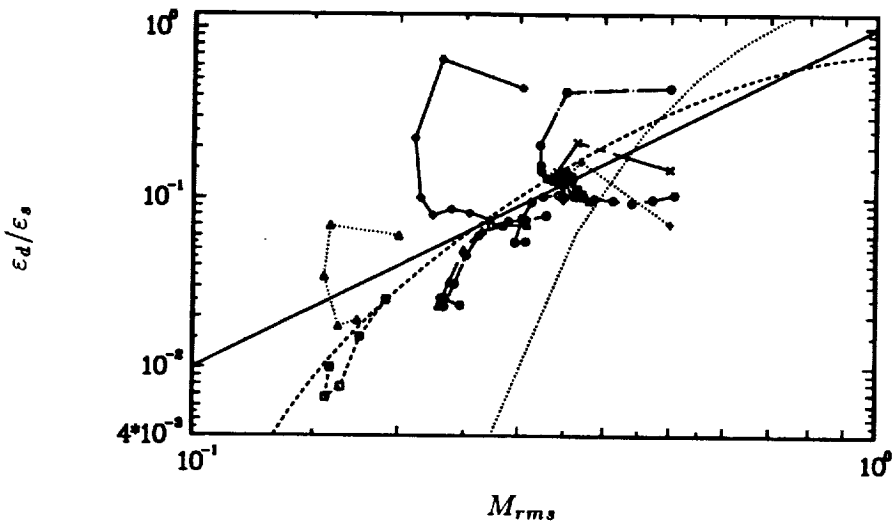

FIGURE 1. Dissipation ratio, $\varepsilon_d/\varepsilon_s$, as a function of M_{rms}. DNS data, symbols; model of Sarkar *et al.* , ——— ; theoretical formulation of Zeman (1991), ····· ; approximate relation of Zeman (1990) given by equation (5), ---- .

DNS data very well, especially at lower values of M_{rms}. This result is surprising in light of the previous comparison made with the DNS data.

In order to clarify the situation we need to examine the theory developed by Zeman (1990, 1991) more closely. There are some acknowledged errors in the form of the PDFs given in Zeman (1990, 1991), and so the development of the theory will be outlined and appropriate corrections made.

Based on scaling arguments, Zeman arrives at equation (5) of Zeman (1990) which can be rewritten as

$$\varepsilon_d' = \left(\frac{q^3}{L}\right) \frac{1}{M_r^{*3}} \left(\frac{(m_1^{*2}-1)}{m_1^*}\right)^3 . \tag{6}$$

This relation gives the contribution to the dilatational dissipation rate from an eddy shocklet structure where $m_1^* = \sqrt{u_i' u_i'}/a^*$ is the instantaneous Mach number on the upstream side of the shock. The Mach number used by Zeman is based on the speed of sound at sonic conditions, $a^* = \sqrt{\gamma R T^*}$. The average dilatational dissipation is obtained from a distribution of eddy shocklet structures, and, therefore, one needs to integrate this expression with the PDF of m_1^*.

Zeman has proposed two forms of the PDF depending on the flow. For homogeneous turbulence, in which case the velocity fluctuations are nearly Gaussian, the proposed PDF is given in equation (5) of Zeman (1991). Results using this PDF are shown in figure 1, and, as discussed above, they do not agree with the DNS data. In order to check whether the disagreement is due to differences between the actual PDF and the model PDF, the PDF of the fluctuating Mach number was taken directly from the simulations. However, the results did not agree with those of the DNS. This suggests that the basic theory does not apply to the flow

conditions considered in the DNS.

For inhomogeneous flows, such as mixing layers, in which the PDF of the velocity fluctuations are non-Gaussian, Zeman (1990) suggests using a Gram-Charlier expansion in which the kurtosis, K, appears as a parameter. The PDF given in equation (6) of Zeman (1990) contains a typographical error. It is also missing a factor of σ and is, therefore, unnormalized. The normalized PDF, put in terms of the Mach number, is

$$p(m^*, K) = \frac{1}{\sqrt{2\pi}\sigma}\left\{1 + \frac{(K-3)}{4!}\left[3 - 6\left(\frac{m^*}{\sigma}\right)^2 + \left(\frac{m^*}{\sigma}\right)^4\right]\right\}\exp\left(-\frac{m*^2}{2\sigma^2}\right) \quad (7)$$

where the variance $\sigma = M_T^*$.

Zeman obtains the average dilatational dissipation rate by integrating the expression in equation (6) with the PDF of m^*. This formulation, given in equation (7) of Zeman (1990), has a factor of $1/M_T^{*4}$ which is correct for the unnormalized PDF. If the PDF is normalized, then the dilatational dissipation rate is given by

$$\varepsilon_d \propto \frac{q^3}{L}\left[\frac{1}{M_T^{*3}}\int_1^\infty \left(\frac{m^{*2}-1}{m^*}\right)^3 p(m^*)\,dm^*\right] . \quad (8)$$

Relating q^3/L to ε_s gives the form shown in equation (3) where $F(M_T^*)$ is the term in the brackets in equation (8) above.

Zeman (1990) used the non-Gaussian PDF given in equation (7) to produce $F(M_T^*)$ for a range of values of the kurtosis K. These results are shown in figure 2 of Zeman (1990). The curve fit given in equation (5) is supposed to correspond roughly to the theoretical predictions with K between 6 and 8. Comparing values of $F(M_T^*)$ from equation (5) with those from the figure, this seems to be the case for most of the range of M_T^*; however, for values of $M_T^* < 0.5$ there are some significant differences. Differences in this range are important because the calculations of a compressible mixing layer done by Zeman (1990) show that M_T^* is limited to values less than 0.5.

In order to make a detailed comparison, the function $F(M_T^*)$ calculated using the PDF from equation (7) is shown in figure 2(a) for values of $K = 4$, 6, 8, 10, along with the model given by equation (5). The curves shown in figure 2(a) do not exactly match those in figure 2 of Zeman (1990). The curves in figure 2(a) are somewhat lower than the corresponding curves from Zeman (1990), but the shapes of the curves are the same. The differences in the curves seem to be greater for higher values of K. The reason for the differences may be the approximations used to evaluate the integral in equation (8). It is believed that the curves in the current paper are accurate.

The model curve shown in figure 2(a) has the same basic S-shape as the theoretical curves, and it lies between the curves for $K = 6$ and $K = 8$ for a large range of Mach numbers; but, in the range $M_T^* < 0.5$, the model curve deviates significantly from the theoretical curves. This is shown in detail in figure 2(b). The model gives

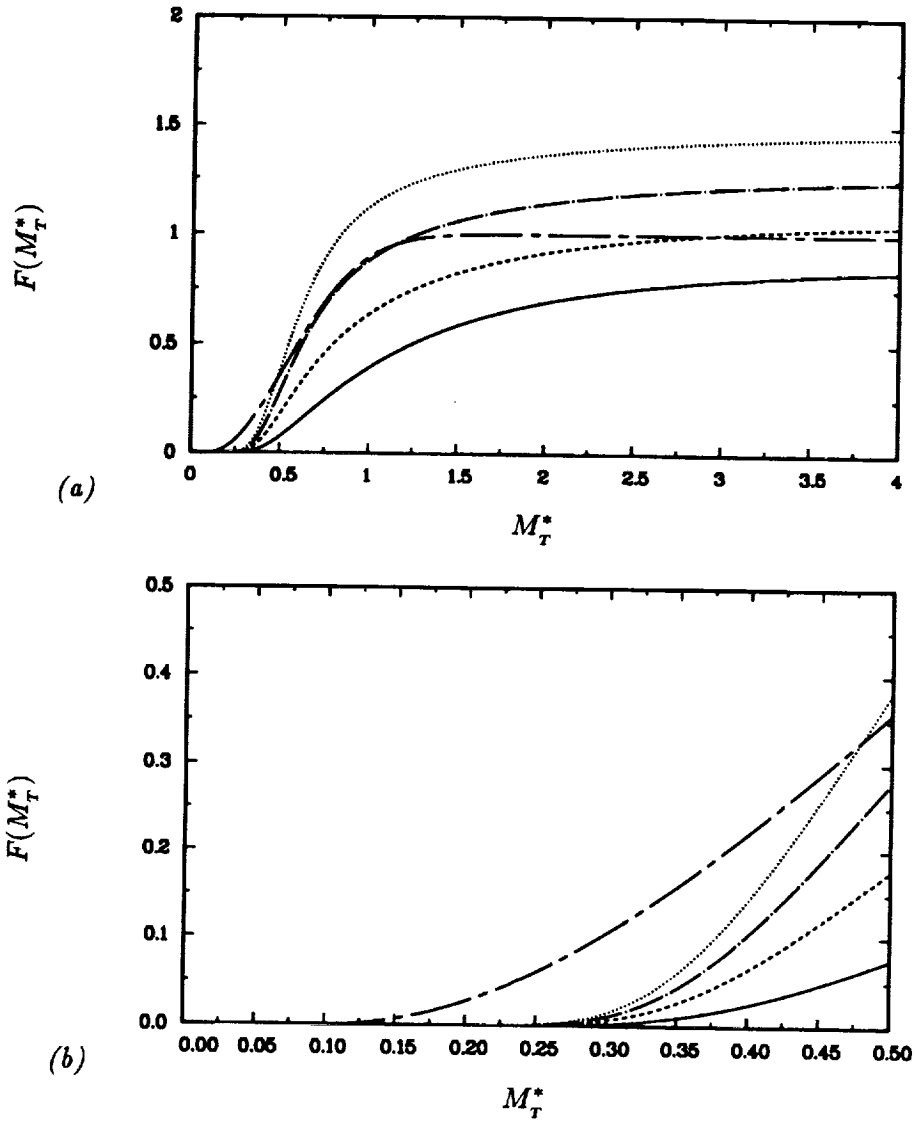

FIGURE 2. Dissipation function $F(M_T^*)$ for various values of K, (a) for a wide range of Mach numbers, (b) for $M_T^* < 0.5$. $K = 4$, ——— ; $K = 6$, - - - - ; $K = 8$, —·— ; $K = 10$, ····· ; approximate relation from equation (5), — — — .

much higher values for $F(M_T^*)$ than what the theory predicts. The differences are especially great at lower values of M_T^*. The implication of the comparison shown in figure 2(b) is that, in the range of Mach numbers where the model is used, the model does not represent the theory upon which it is based. This does not mean that the model is not useful — it has been used to give the correct decrease in mixing layer thickness with increasing convective Mach number. However, the model must be viewed correctly as an empirical fit rather than having a fundamental theoretical

basis. The eddy shocklet dissipation theory developed by Zeman (1990) may still be valid under flow conditions different than those discussed here.

Returning to the comparison done by Viegas & Rubesin, one can understand the relative performance of the models of Zeman and Sarkar *et al.* in the compressible mixing layer by comparing the values predicted for ϵ_d/ϵ_s. From figure 4 of Zeman (1990), compressibility effects become important for convective Mach numbers above 0.5, and, from figure 5 of that paper, this corresponds to $M_T^* > 0.3$. From figure 1 of the current paper, Zeman's model gives a greater value of ϵ_d/ϵ_s than Sarkar's model in the range $0.25 < M_{rms} < 0.75$. So, in the range of Mach numbers where compressibility effects are important, Zeman's model predicts a higher dissipation rate than Sarkar's model. Therefore, while Zeman's model gives the correct growth rate, Sarkar's model predicts too large a growth rate. However, it should be pointed out that the comparison of Viegas & Rubesin only included as extra compressibility terms the dilatational dissipation rate and neglected the pressure-dilatation and the inhomogeneous term arising from the pressure-velocity correlation. Also, the mixing layer may have compressibility effects that reduce the production rate. These additional effects have been lumped into the evaluation of the dilatational dissipation rate models.

Let us now examine how the DNS data fits into the evaluation of the models. From figure 1, Zeman's model agrees very well with the DNS data at the lower values of M_{rms}, while Sarkar's model overpredicts the dissipation rate in this range. The differences in the models for low turbulent Mach numbers are not significant for the mixing layer; however, there may be other flows, such as boundary layers, where these differences are important. For $M_{rms} > 0.3$, there are large differences between the DNS data and the models. The value of ϵ_d/ϵ_s from the DNS becomes roughly constant at 0.09 for $M_{rms} > 0.3$. This trend is not predicted by either model. Since Zeman's model agrees with the experimental results on mixing layers, there are most likely physical differences in the mechanism of the dilatational dissipation rate between mixing layers and homogeneous shear flow. The dilatational dissipation within homogeneous turbulent shear flow is examined in more detail in the next section.

3. Cause of the dilatational dissipation in homogeneous shear flow

In Blaisdell *et al.* (1992), flow fields from DNS of compressible homogeneous turbulence were examined in order to see the effects of compressibility. Eddy shocklets were found, which are regions of high local dilatational dissipation rate. However, these structures do not necessarily contribute significantly to the average dilatational dissipation rate because they are also highly intermittent. Nonetheless, it was believed that eddy shocklets are important to the dynamics of the dilatational dissipation rate. Also, a mechanism for the generation of eddy shocklets was suggested in which streamwise vortical structures cause high speed and low speed fluid to come into contact, creating a compression that leads to the shock. In the current work, the question of the importance of eddy shocklets to the dilatational dissipation rate is reexamined, and, by using flow visualization of the temporal evolution of

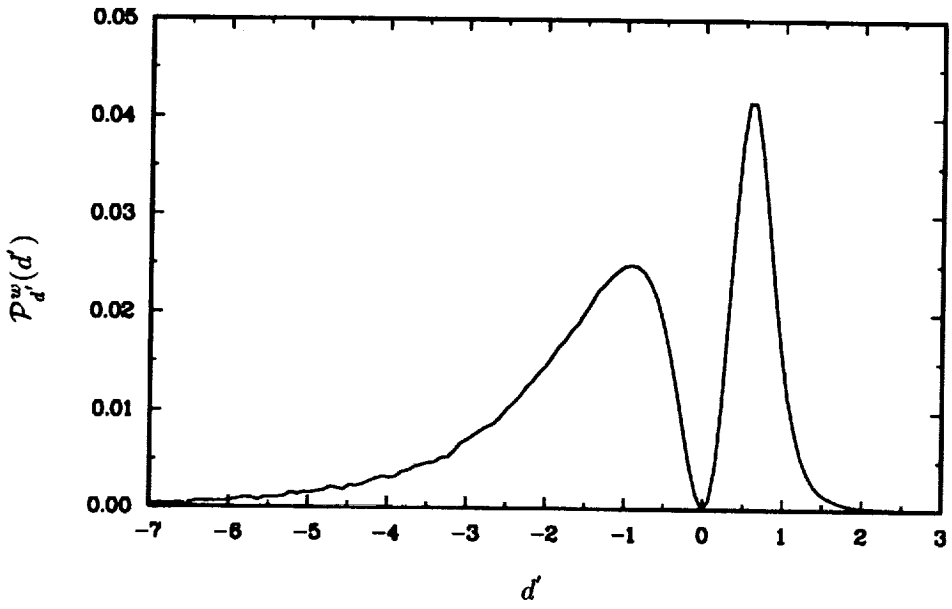

FIGURE 3. Weighted PDF of the dilatation for simulation scb192 at $St = 12$.

the turbulence, a different mechanism for the generation of eddy shocklets is shown to occur.

The nature of the dilatational dissipation rate can best be found by identifying the regions of the flow that contribute the most to the dilatational dissipation rate and seeing how these regions evolve in time. In Blaisdell *et al.* (1992), the flow field from simulation scb192 was examined at the nondimensional time $St = 12$. In the current study, we consider the time evolution of the turbulence using flow fields from the same simulation for times between $St = 11$ and 12.

In order to determine which regions of the flow contribute most significantly to the dilatational dissipation rate, use is made of a weighted PDF of the dilatation formed by Blaisdell *et al.* which is defined by

$$\mathcal{P}^w_{d'}(d') = \frac{d'^2 \mathcal{P}_{d'}(d')}{\int_{-\infty}^{\infty} d'^2 \mathcal{P}_{d'}(d')\, dd'} \tag{9}$$

where $\mathcal{P}_{d'}(d')$ is the PDF of the dilatation. Figure 3 shows $\mathcal{P}^w_{d'}(d')$ for simulation scb192 at $St = 12$. The integral of $\mathcal{P}^w_{d'}(d')$ gives the fraction of the dilatational dissipation due to a specific range of values of the dilatation. More of the dilatational dissipation rate comes from negative values of the dilatation, which correspond to compression zones, than from positive values, which correspond to expansion zones. This is consistent with the negative skewness of the dilatation and the fact that the second law of thermodynamics precludes expansion shocks. There are two peak values of $\mathcal{P}^w_{d'}(d')$, one negative at $d' = -0.93$ and one positive at $d' = 0.56$. We will examine the regions where the negative peak values occur since they are associated with compression zones and will give us insight into the formation of eddy shocklets.

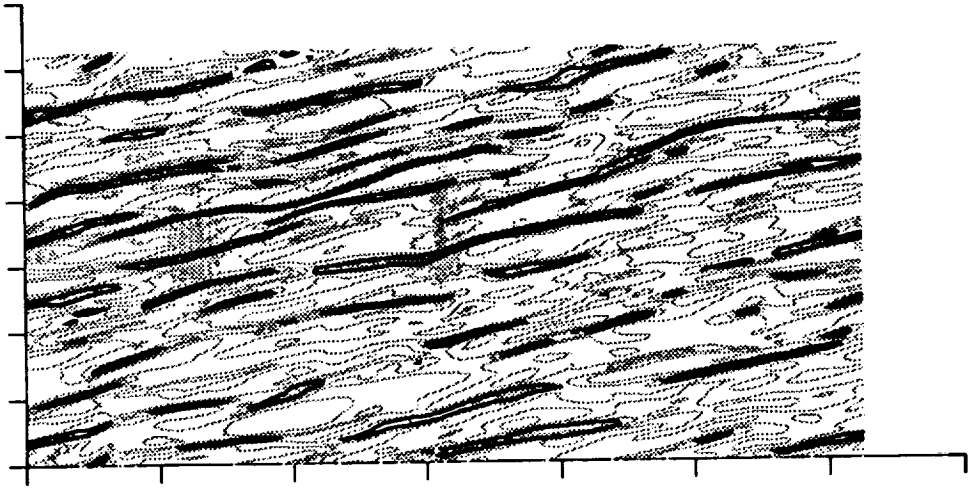

FIGURE 4. Contours of divergence of velocity in an x-y plane for simulation scb192 at $St = 12$. The highlighted contour corresponds to the negative peak in $\mathcal{P}^w_{d'}$.

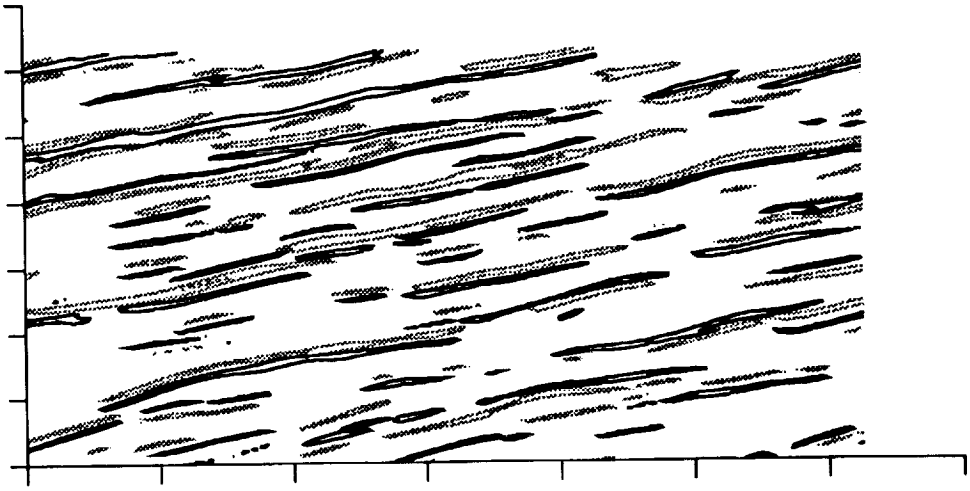

FIGURE 5. The highlighted contour of divergence of velocity at $St = 11.01$ (dark) and $St = 11.26$ (light).

Figure 4 shows contours of the dilatation in an x-y plane for simulation scb192 at $St = 12$. The mean velocity is in the x direction, and the mean velocity gradient is in the y direction. The contour with the peak value of $\mathcal{P}^w_{d'}(d')$ for negative d' is highlighted. The view shown is chosen so that the strongest eddy shocklet (measured by the most negative dilatation) occurs in the center of the frame. The highlighted contour occurs on the periphery of the eddy shocklet but also throughout the rest of the flow field. The regions which contribute most significantly to the dilatational dissipation rate are long and thin and lie at a small positive angle to the direction of the mean flow.

Considerable insight is gained by observing the temporal evolution of these regions. Figure 5 shows the same highlighted contour at two different times, $St = 11.01$ and $St = 11.26$. For this view, the effect of the mean velocity was removed so that any motion observed occurs relative to the mean flow. It is apparent that the regions which contribute to the dilatation propagate as waves. Thus it appears that these regions are associated with large scale acoustic waves.

Next consider the dilatation in a spanwise, z-y plane. Figure 6 shows the spanwise plane at $St = 12$ which cuts through the strongest part of the eddy shocklet shown in figure 4. The same contour of the dilatation is highlighted. The regions that contribute to the dilatational dissipation rate are for the most part broad and thin. This view together with those shown in figures 4 and 5 gives the impression that these regions are portions of plane waves.

Again, it is useful to observe the temporal evolution of the regions that contribute the most to the dilatational dissipation rate. Figure 7 shows a sequence of the highlighted d' contour superposed on contours of streamwise vorticity for times between $St = 11$ and 12. The highlighted contours propagate as plane waves as shown before.

In figure 6, the eddy shocklet occurs about three quarters of the way across the plane (in z) and half way up (in y) at the base of the V-shaped highlighted contour. It is fairly narrow in the spanwise direction. The formation of the eddy shocklet can be observed by following the highlighted contour in figure 7(a) which lies somewhat below the location of that pointed out in figure 6 and which extends about a third of the way across the computational domain. As the contour propagates upward, it is distorted. It is believed that this distortion is due mainly to the vortical part of the turbulence, which is the reason for including contours of streamwise vorticity in figure 7. Shaded contours show positive streamwise vorticity, while dashed contours show negative streamwise vorticity. The particular contour of interest gets distorted as it passes what appears to be a pair of counter rotating streamwise vortices. Once the contour is distorted, it becomes focused and forms a cusp which is where the eddy shocklet occurs. Thus, the eddy shocklet is formed by a focused acoustic wave.

We have seen that the dilatational dissipation within homogeneous shear flow is associated mainly with large scale acoustic waves. Eddy shocklets do form, but, because they are highly intermittent, they do not contribute significantly to the dissipation.

The view shown in figure 4 with the highlighted contours lying at a shallow angle suggests that the regions which contribute the most to the dilatational dissipation may be due to the kinematic tilting of acoustic waves by the mean velocity field. Tilted acoustic waves would have increased dissipation compared to that of simple acoustic waves. This mechanism could be investigated by flow visualization, but this was not done.

The possible tilting of acoustic waves points out one of the differences between homogeneous flows and inhomogeneous flows such as mixing layers. In homogeneous shear flow, the shear continually acts on the turbulence, and any acoustic waves will feel the effect of the shear as long as they exist. In a mixing layer, acoustic waves

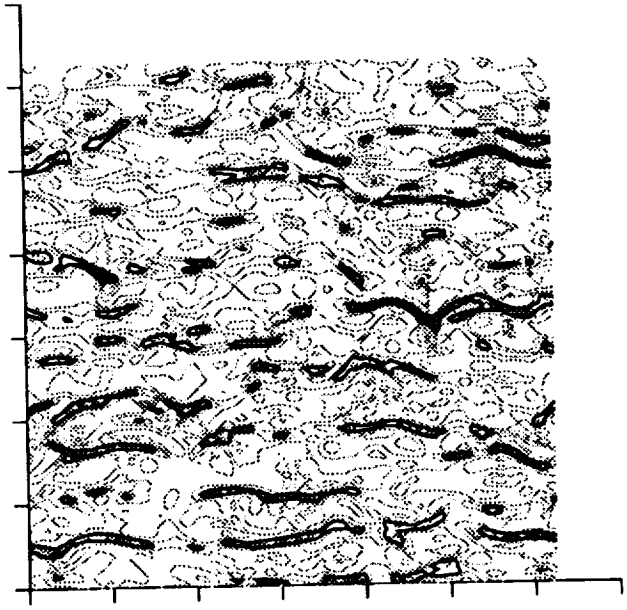

FIGURE 6. Contours of divergence of velocity in a z-y plane in simulation scb192 at $St = 12$. The highlighted contour corresponds to the negative peak in $\mathcal{P}_{d'}^{w}$.

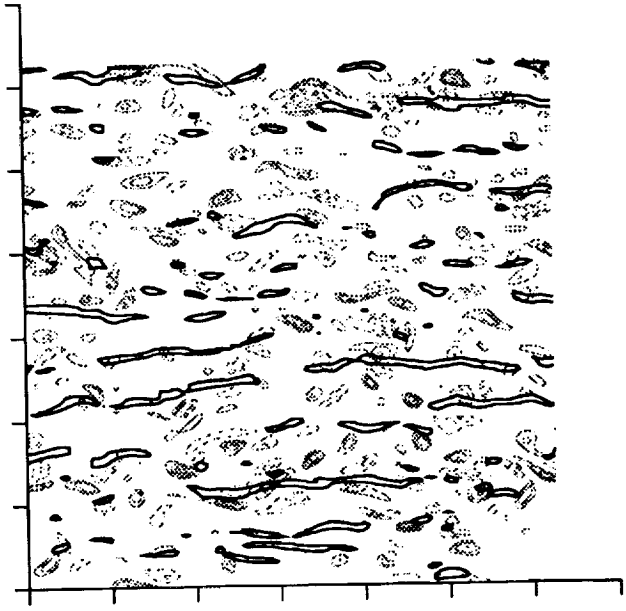

(a) $St = 11.01$

FIGURE 7. Sequence of views showing the highlighted contours of divergence of velocity superposed on contours of streamwise vorticity (shaded contours, positive ω_x; dashed contours, negative ω_x). (a) $St = 11.01$, (b) $St = 11.26$, (c) $St = 11.50$, (d) $St = 11.75$, (e) $St = 12$.

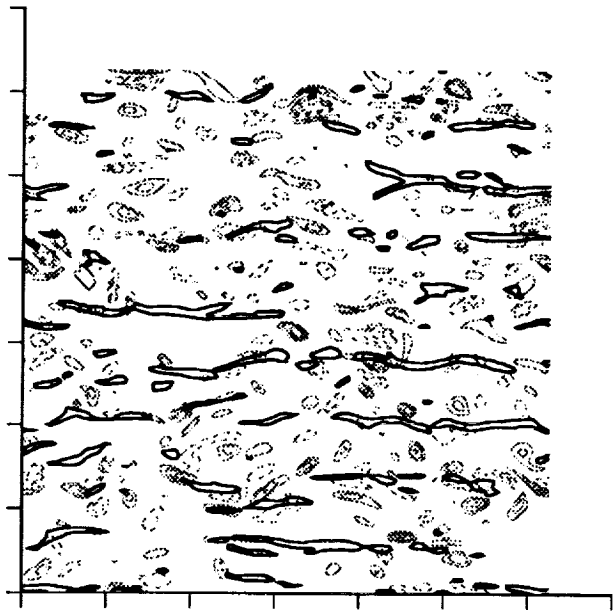

(b) $St = 11.26$

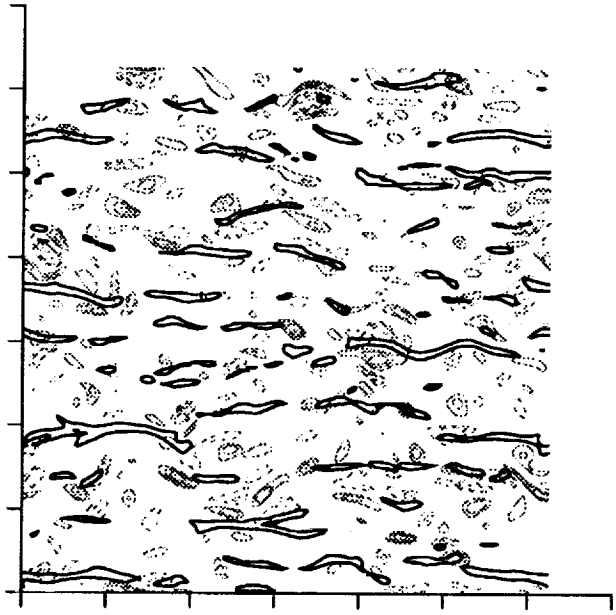

(c) $St = 11.50$

FIGURE 7. (continued).

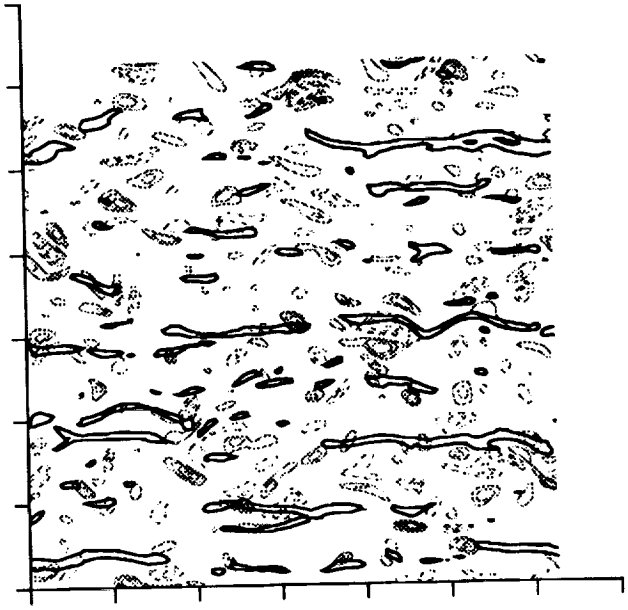

(d) $St = 11.75$

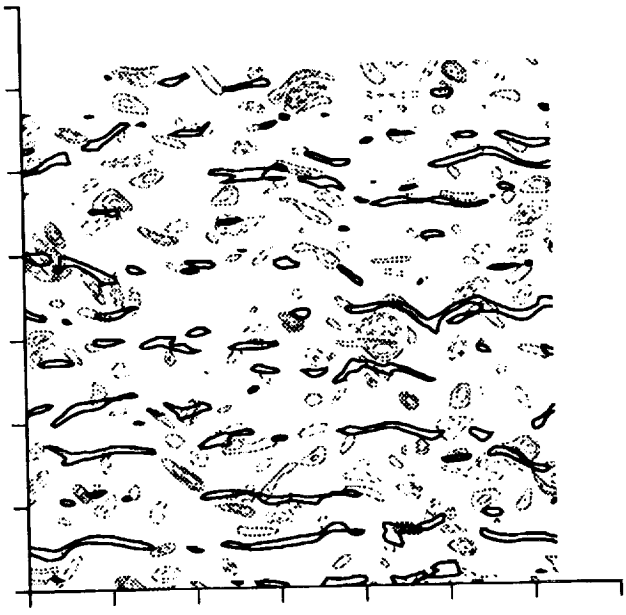

(e) $St = 12$

FIGURE 7. (continued).

have the chance to propagate to the freestreams. The mean shear in a mixing layer will act on acoustic waves, but the interaction will only be significant if the time scale of the mean shear is small compared to time scale for an acoustic wave to propagate out of the layer. The propagation of acoustic waves to the freestream represents a loss of turbulent kinetic energy which is separate from the dilatational dissipation. Perhaps compressible turbulence models should be formulated to account for the separate mechanisms.

4. Conclusions

The dilatational dissipation within compressible homogeneous turbulent shear flow has been investigated using data and flow visualizations from direct numerical simulations. It is found that the dilatational dissipation rate is associated with large scale acoustic waves. Eddy shocklets, which are regions of large local dilatational dissipation, are observed; however, they occur too infrequently to contribute significantly to the average dilatational dissipation rate. A mechanism for the formation of eddy shocklets is shown to be the focusing of large scale acoustic waves.

The turbulence models for the dilatational dissipation rate of Zeman (1990, 1991) and Sarkar *et al.* (1991) were investigated. The model of Sarkar *et al.* agrees well with the DNS data for values of the turbulent Mach number less than 0.3. Some confusion arose concerning the formulation of Zeman's model. It was found that an approximate relation used for the case of mixing layers does not accurately represent the theory upon which the model is based. The theoretical formulation does not agree with the DNS data, while the approximate relation shows very good agreement for turbulent Mach numbers less than 0.3. For turbulent Mach numbers above 0.3, there are large differences between the DNS data and the models. Since Zeman's model was developed for a mixing layer and works well for that case, the differences between the DNS data and the models may be due to the differences in the physical nature of compressible homogeneous shear flow and a compressible mixing layer.

REFERENCES

BLAISDELL, G. A., MANSOUR, N. N., & REYNOLDS, W. C. 1991 Numerical simulations of compressible homogeneous turbulence. *Report TF-50.* Mechanical Engineering, Stanford University.

BLAISDELL, G. A., MANSOUR, N. N., & REYNOLDS, W. C. 1992 Compressibility effects on the growth and structure of homogeneous turbulent shear flow. Submitted to J. Fluid Mech.

SARKAR, S., ERLEBACHER, G., & HUSSAINI, M. Y. 1991a Direct simulation of compressible turbulence in a shear flow. *Theoret. Comput. Fluid Dynamics.* **2,** 291-305.

SARKAR, S., ERLEBACHER, G., HUSSAINI, M. Y., & KREISS, H. O. 1991b The analysis and modelling of dilatational terms in compressible turbulence *J. Fluid Mech..* **227,** 473-493.

SARKAR, S. 1992 The pressure-dilatation correlation in compressible flows. Submitted to Phys. Fluids A.

VIEGAS J. R. & RUBESIN, M. W. 1991 A comparative study of several corrections to turbulence models applied to high-speed shear layers. *AIAA paper 91-1783.*

ZEMAN O. 1990 Dilatation dissipation: The concept and application in modeling compressible mixing layers. *Phys. Fluids A.* **2,** 178-188.

ZEMAN O. 1991 On the decay of compressible isotropic turbulence. *Phys. Fluids A.* **3,** 951-955.